Materials Transactions, Vol. 42, No. 8 (2001) pp. 1588 to 1592
Special Issue on Nano-Metals I

Mg-Based Hydrogen Storage Materials with Improved Hydrogen Sorption

Wolfgang Oelerich, Thomas Klassen and Rüdiger Bormann

GKSS Research Center Geesthacht GmbH, D-21502 Geesthacht, Germany

Nanocrystalline MgH_2/Me_xO_y composite powders were produced by high energy ball milling (Me_xO_y = Sc_2O_3, TiO_2, V_2O_5, Cr_2O_3, Mn_2O_3, Fe_3O_4, CuO, Al_2O_3, SiO_2). The hydrogen absorption and desorption kinetics were determined in view of a technical application. The addition of selected oxides lead to an enormous catalytic acceleration of hydrogen sorption compared to pure nanocrystalline hydrides. In absorption, the catalytic effect of TiO_2, V_2O_5, Cr_2O_3, Mn_2O_3, Fe_3O_4, and CuO is comparable. Concerning desorption, the composite material containing Fe_3O_4 shows the fastest kinetics followed by V_2O_5, Mn_2O_3, Cr_2O_3 and TiO_2. Only 0.2 mol% of the catalysts is sufficient to provide a fast sorption kinetics. Additionally, Mg absorbs hydrogen already at room temperature by the use of metal oxides as catalysts. Furthermore, it is demonstrated for the first time that MgH_2/Me_xO_y-powders release hydrogen at 200°C.

(Received February 20, 2001; Accepted April 2, 2001)

Keywords: *high energy ball milling, nanocrystalline microstructure, hydrogen storage, magnesium hydride, catalysis, metal oxide catalyst*

1. Introduction

Hydrogen is the ideal means of storage, transport and conversion of energy for a comprehensive clean-energy concept. Regarding the use of hydrogen as fuel for the zero-emission vehicle, the main problem is the storage of hydrogen. Metal hydrides offer a safe alternative to storage in compressed or liquid form. In addition, metal hydrides have the highest storage capacity by volume. Mg hydride has also a high storage capacity by weight and is therefore favored for mobile applications. However, light metal hydrides have not been considered competitive because of their rather sluggish sorption kinetics. Filling a tank could take several hours. *e.g.*, magnesium hydride needs to be heated up to more than 300°C to obtain relevant sorption properties.[1–4] Therefore, many attempts have been made to qualify magnesium hydride for application by improving the absorption and desorption behavior of the material. Recently, a breakthrough in hydride technology was achieved by preparing nanocrystalline hydrides using high energy ball milling.[5–12] Nanocrystalline magnesium hydride shows indeed a fast absorption kinetics with a loading time of few minutes at 300°C. However, desorption and absorption at lower temperatures are still too slow limiting technical applications.[13] With respect to absorption, this is due to the bad dissociation ability of metallic Mg for hydrogen molecules, because the probability of the adsorption of a H_2-molecule on the Mg-surface is only 10^{-6}.[14] To overcome this problem, catalysts have to be added to magnesium. As has been shown in the past, Pd, Ni, and Fe can be used for a better H_2-dissociation at the surface, *e.g.* for Mg_2Ni, FeTi or $LaNi_5$.[2,15–18] Especially for microcrystalline Magnesium, Tanguy *et al.* have demonstrated that also the addition of V and Ti cause a catalytic acceleration of the hydrogen absorption.[19] Recently, the effect of transition metals (Ti, V, Mn, Fe, Ni) on nanocrystalline Mg has been investigated by Liang *et al.*[20,21] They show that ball milled MgH_2 with additions of 5 at% of the transition metal absorbs at room temperature (1 MPa) and desorbs at 235°C (0.015 MPa). In the present work, we have investigated the influence of cheap metal oxides (Sc_2O_3, TiO_2, V_2O_5, Cr_2O_3, Mn_2O_3, Fe_3O_4, CuO, Al_2O_3, and SiO_2) on the sorption behavior of nanocrystalline Mg-based systems. Special emphasis is put on the sorption kinetics at reduced temperatures, ranging from 300°C down to room temperature.

2. Experimental

The milling experiments were performed with a Fritsch P5 planetary ball mill using hardened Cr-steel milling tools and an initial ball-to-powder weight ratio of 400 g : 40 g. The initial MgH_2 powder (95+%, Goldschmidt GmbH, Germany) was pre-milled for 20 h. Afterwards, different metal oxides (99.9+% metal) were added in the desired overall ratio, and milled for further 100 h. All handling of the powders, including milling, was performed inside a glove box under a continuously purified Ar atmosphere (oxygen, and water content each below 1 ppm). For characterization of the sorption properties, specimen holders were sealed inside the box and attached to a hydrogen titration apparatus, that was especially designed for fast data acquisation (Hydro-Québec, patent pending[22]). Kinetic measurements were performed between 25 and 300°C. The pressure of hydrogen (purity 99.993%) was 8.4 bar for absorption. For measurements of the desorption kinetics, the chamber was evacuated. The weight of each specimen was about 150 mg.

The hydrogen desorption rates of the materials are determined by using the time for desorption between 80 and 20% of the maximum hydrogen capacity. The desorption rate obtained in this way with a unit of mass%-H_2 per second ($\Delta c_H/\Delta t$) is converted to a desorption rate with the unit kW per kg of the material by using the intrinsic heat value of hydrogen being 120 kJ/g.

3. Results and Discussion

In Figs. 1 and 2 the absorption and desorption curves of the materials $MgH_2/(CuO)_{0.05}$, $MgH_2/(Mn_2O_3)_{0.05}$, $MgH_2/(Cr_2O_3)_{0.05}$, $MgH_2/(Fe_3O_4)_{0.05}$ as well as $MgH_2/$

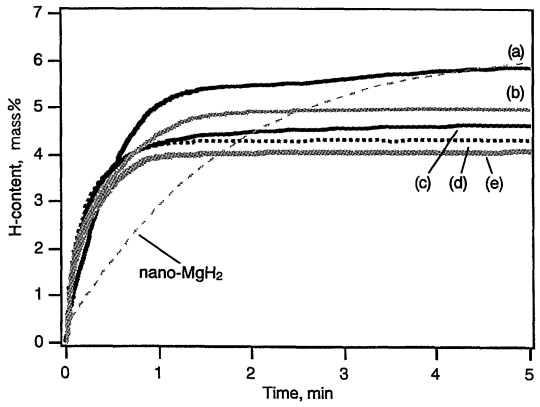

Fig. 1 Hydrogen absorption curves of $MgH_2/(Me_xO_y)_{0.05}$ composites at 300°C under a hydrogen pressure of 0.84 MPa bar. (a) $MgH_2/(CuO)_{0.05}$; (b) $MgH_2/(Mn_2O_3)_{0.05}$; (c) $MgH_2/(Cr_2O_3)_{0.05}$; (d) $MgH_2/(Fe_3O_4)_{0.05}$; (e) $MgH_2/(V_2O_5)_{0.05}$.

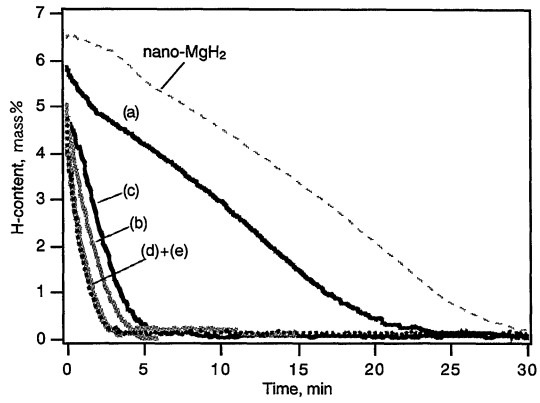

Fig. 2 Hydrogen desorption curves of $MgH_2/(Me_xO_y)_{0.05}$ composites at 300°C in vacuum. (a) $MgH_2/(CuO)_{0.05}$; (b) $MgH_2/(Mn_2O_3)_{0.05}$; (c) $MgH_2/(Cr_2O_3)_{0.05}$; (d) $MgH_2/(Fe_3O_4)_{0.05}$; (e) $MgH_2/(V_2O_5)_{0.05}$.

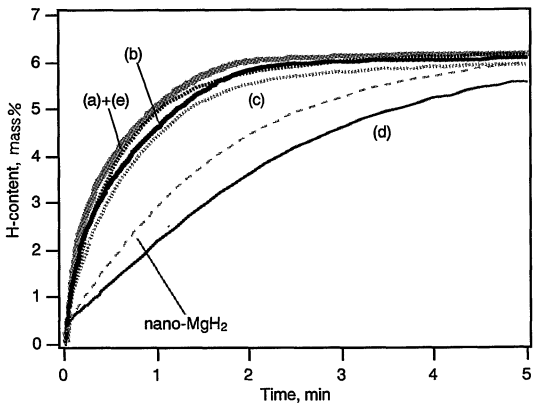

Fig. 3 Hydrogen absorption curves of $MgH_2/(Me_xO_y)_{0.05}$ composites at 300°C under a hydrogen pressure of 0.84 MPa bar. (a) $MgH_2/(V_2O_5)_{0.01}$; (b) $MgH_2/(TiO_2)_{0.01}$; (c) $MgH_2/(Al_2O_3)_{0.01}$; (d) $MgH_2/(SiO_2)_{0.01}$; (e) $MgH_2/(Sc_2O_3)_{0.01}$.

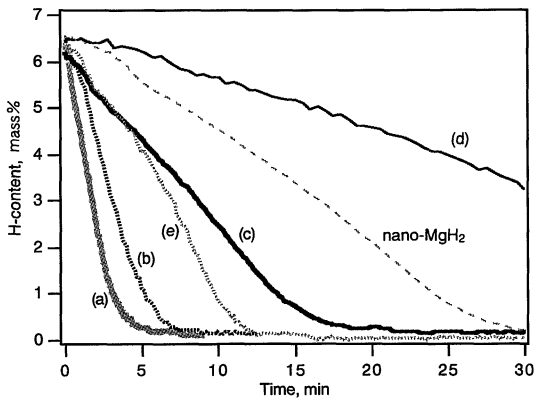

Fig. 4 Hydrogen desorption curves of $MgH_2/(Me_xO_y)_{0.05}$ composites at 300°C in vacuum. (a) $MgH_2/(V_2O_5)_{0.01}$; (b) $MgH_2/(TiO_2)_{0.01}$; (c) $MgH_2/(Al_2O_3)_{0.01}$; (d) $MgH_2/(SiO_2)_{0.01}$; (e) $MgH_2/(Sc_2O_3)_{0.01}$.

$(V_2O_5)_{0.05}$, each with a metal oxide content of 5 mol%, are presented and compared to MgH_2 without any catalyst additions. As can be seen clearly, the addition of metal oxides leads to a notable enhancement of both the absorption and desorption kinetics. The absorption kinetics is about the same for these materials at 300°C and the maximum hydrogen content is typically reached after 2 min. Differences regarding the maximum hydrogen capacity are related to the different densities of the oxides. For CuO (curve a), the shape of the absorption curve is different (in particular between 2 and 5 min). Absorption takes place in two distinct steps: in the first step, the material reaches a plateau capacity of 5.5 mass%. Afterwards, the hydrogen content rises again slightly up to 6 mass%. In comparison with pure MgH_2 the catalytic effect of oxide additions is especially pronounced upon desorption. Desorption is already completed after 3 to 5 min for most of the oxides, with Fe_3O_4 and V_2O_5 yielding the fastest desorption kinetics. In the case of CuO, the desorption kinetics also differs from the other oxides. The material $MgH_2/(CuO)_{0.05}$ needs around 25 min for a full release of hydrogen.

Furthermore, the catalytic effect of the oxides Sc_2O_3, TiO_2, Al_2O_3 and SiO_2 was investigated. Figure 3 shows the absorption curves of the materials $MgH_2/(Sc_2O_3)_{0.01}$, $MgH_2/(TiO_2)_{0.01}$, $MgH_2/(Al_2O_3)_{0.01}$ and $MgH_2/(SiO_2)_{0.01}$ in comparison with $MgH_2/(V_2O_5)_{0.01}$. While the first three composites reach similar absorption kinetics as $MgH_2/(V_2O_5)_{0.01}$, SiO_2 slows down the kinetics even in comparison to pure nanocrystalline MgH_2. Upon desorption, a good catalytic effect is obtained with the alloy additions TiO_2 and V_2O_5. Hydrogen is fully desorbed within 7 min. Sc_2O_3 has only a minor, Al_2O_3 and SiO_2 have no accelerating effect on the hydrogen release (Fig. 4).

To study the effect of different amounts of catalyst, the MgH_2/Cr_2O_3 system was taken as an example (Figs. 5 and 6). The overall capacities differ in accordance with the particular amounts of catalyst. The full capacities of 4.7, 6.0, and 6.7 mass% hydrogen are achieved for oxide contents of 5, 1, and 0.2 mol%, respectively, within 2 min at 300°C. For comparison: pure nanocrystalline MgH_2 reaches 3.9 mass% within 2 min. The initial absorption rates between 1 and 3 mass% are 218 kW/kg for the MgH_2/Cr_2O_3 systems and 35 kW/kg for pure MgH_2, respectively. The calculated absorption rates demonstrate that the absorption kinetics of the MgH_2/Cr_2O_3 systems do not depend on the catalyst content in the range investigated. This means that the capacity of the material can be increased significantly without making compromises with respect to absorption kinetics. Similarly, a decrease of the oxide content also has no influence on the release rate of hydrogen. Figure 6 presents the desorption curves for

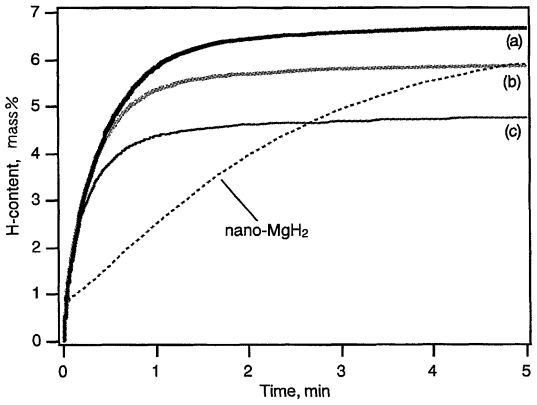

Fig. 5 Hydrogen absorption curves of MgH_2/Cr_2O_3-composites with different oxide contents at 300°C under a hydrogen pressure of 0.84 MPa bar. Cr_2O_3-content: (a) 0.2 mol%; (b) 1 mol%; (c) 5 mol%.

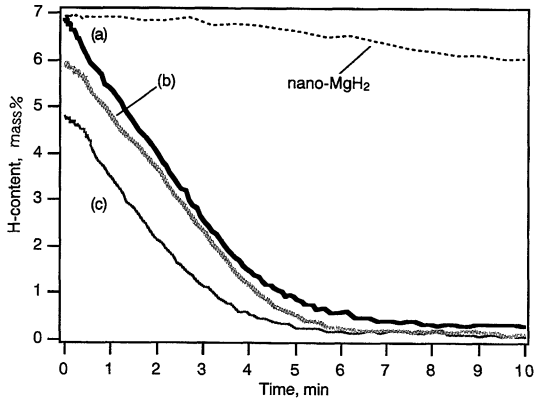

Fig. 6 Hydrogen desorption curves of MgH_2/Cr_2O_3-composites with different oxide contents at 300°C in vacuum. Cr_2O_3-content: (a) 0.2 mol%; (b) 1 mol%; (c) 5 mol%.

Mg containing 5, 1, and 0.2 mol%Cr_2O_3. The desorption rate is determined to 23 kW/kg and does not depend on the catalyst content. The desorption process is complete after 6 to 8 min, depending on the starting capacity. Hence, for a technical application of a storage tank on the basis of MgH_2/Cr_2O_3 a small catalyst content of 0.2 mol% (*i.e.* 0.3 vol% or 1.1 mass%) is sufficient to achieve both fast absorption and desorption kinetics.

The desorption rates of the different MgH_2/Me_xO_y-systems are summarized in Fig. 7. While the addition of CuO, Al_2O_3, Sc_2O_3, and SiO_2 causes only a little change in the desorption rate in comparison to nanocrystalline pure MgH_2, the oxides of the transition metals Ti, V, Cr, Mn, and Fe lead to significantly enhanced hydrogen sorption kinetics. The highest desorption rates are achieved with Fe_3O_4 (40 kW/kg) and V_2O_5 (33 kW/kg).

For a technical application it is interesting to investigate, whether metal oxide additions are also favorable at lower temperatures. Figure 8 shows absorption curves at 300 and 100°C for the systems MgH_2/Cr_2O_3 and MgH_2/Fe_3O_4 each with a catalyst content of 0.2 mol% in comparison to pure MgH_2. At 100°C and a hydrogen pressure of 0.84 MPa pure nanocrystalline MgH_2 absorbs 1.3 mass% within 10 min. In contrast, $MgH_2/(Fe_3O_4)_{0.002}$ takes up double as much hydrogen, *i.e.* 2.5 mass%, and $MgH_2/(Cr_2O_3)_{0.002}$ absorbs 2.9 mass% under the same conditions. A further reduction of the absorption

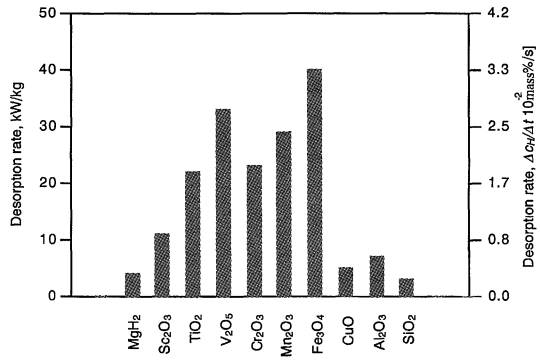

Fig. 7 Desorption rates of the investigated material systems MgH_2/Me_xO_y at 300°C in comparison to nanocrystalline pure MgH_2.

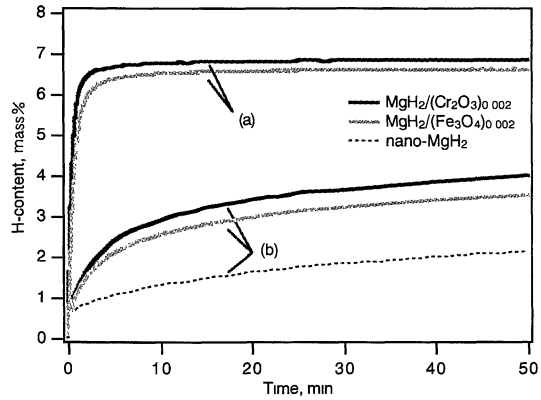

Fig. 8 Hydrogen absorption curves of $MgH_2/(Me_xO_y)_{0.002}$-composites in comparison to pure nanocrystalline MgH_2 under a hydrogen pressure of 0.84 MPa bar: $T = 300$°C (a); $T = 100$°C (b).

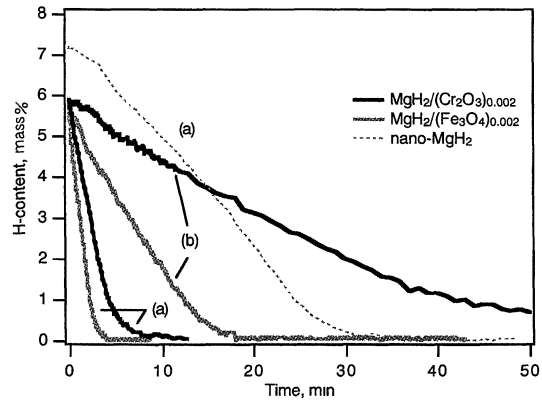

Fig. 9 Hydrogen desorption curves of $MgH_2/(Me_xO_y)_{0.002}$-composites in comparison to pure nanocrystalline MgH_2 in vacuum: $T = 300$°C (a); $T = 250$°C (b).

temperature is possible, as shown in Fig. 10. With the addition of chromium oxide absorption is observed also at room temperature with superior rates over carbon nanotubes (after Ref. 23)). Furthermore, desorption temperatures can also be reduced (Fig. 9). Whereas pure nanocrystalline MgH_2 does not desorb any hydrogen at 250°C in quantitative manner, desorption is possible even at 200°C using oxide catalysts (Figs. 9(b) and 11). With 0.2 mol%Cr_2O_3, a desorption rate of 3 kW/kg is reached at 250°C. This value is comparable to pure nanocrystalline MgH_2 at 300°C (Fig. 7). The desorption rate is more than double as high for the addition of Fe_3O_4 (8 kW/kg). The experimental results point out that the best

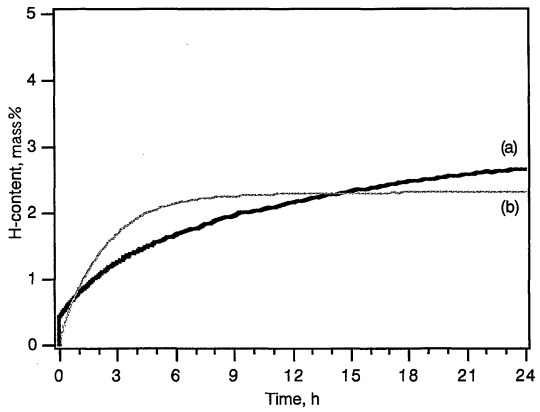

Fig. 10 Hydrogen absorption curve of $MgH_2/(Cr_2O_3)_{0.05}$-composites at $T = 25°C$ under a hydrogen pressure of 0.84 MPa bar (a), and, for comparison, experimental results for carbon nanotubes at $T = 25°C$, $p = 9.5$ Mpa (after Ref. 23)).

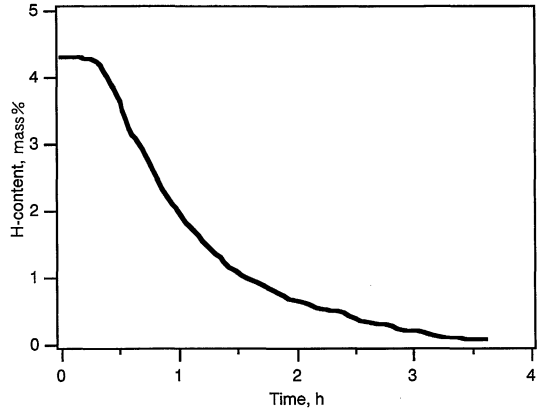

Fig. 11 Hydrogen desorption curve of $MgH_2/(Cr_2O_3)_{0.05}$-composites at $T = 200°C$ in vacuum.

catalytic effect upon absorption is achieved for Cr_2O_3, while Fe_3O_4 yields a faster desorption kinetics. Therefore, good results for both absorption and desorption of hydrogen can be expected if these two oxides are combined. More details can be found in.[24)]

With respect to both, capacity and kinetics, the storage materials are superior to current requirements (Fig. 12), even at 250°C, if lower pressure can be tolerated.[25)] Regarding kinetics, only nanocrystalline Mg with $LaNi_5$ as a catalyst is faster. However, this Mg/$LaNi_5$ composite looses its fast kinetics upon cycling, because it decomposes into the equilibrium phases Mg, Mg_2Ni and LaH_3.[26)] With respect to long term cycling stability, the properties of Mg with oxide catalysts after 1000 cycles were also investigated (Fig. 13). Kinetics slow down by less than a factor of two, which still exceeds the requirements by a factor of 100. The capacity is only decreased from 7 mass% to about 6.6 mass% hydrogen, which is 5 times better than commercial rechargeable battery cells. Details will be published in a forthcoming paper.[27)]

It is yet unclear, what the actual mechanism of catalysis for hydrogen sorption is. In further studies of our group, the advantages of using cheap metal oxides, carbides, and nitrides as catalysts have been compared to the catalytic effect of the respective pure metal. *e.g.*, unlike the pure metallic V, the V-containing compounds V_2O_5, VN, and VC act as catalysts for the magnesium-hydrogen reaction. V_2O_5 yields the

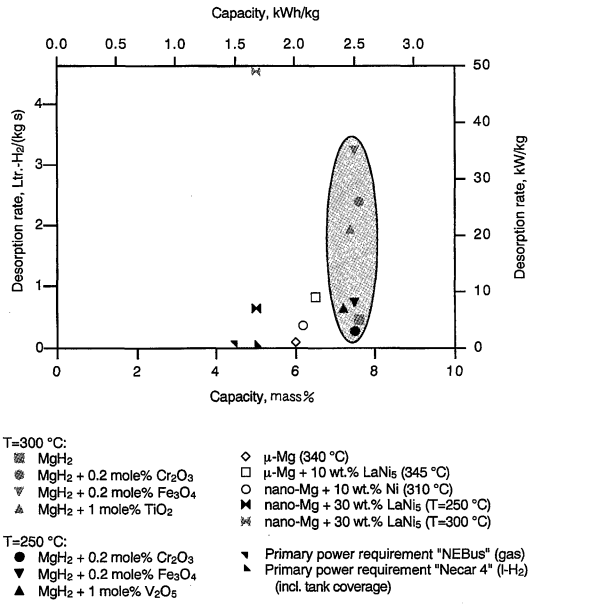

Fig. 12 Comparison between literature data,[2,19–21,26,33)] primary power data for the Daimler Chrysler prototypes[28)] and results of this work (highlighted) with respect to capacity and desorption rate.

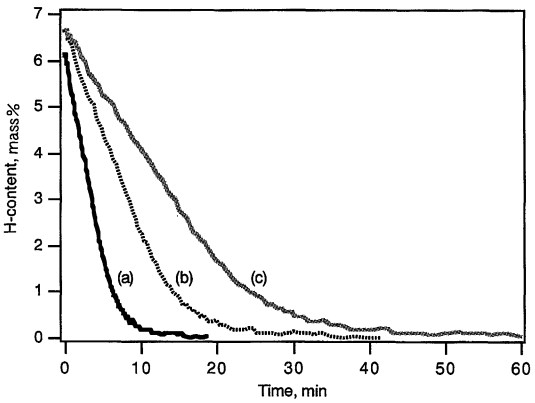

Fig. 13 Hydrogen desorption curves of $MgH_2/(Cr_2O_3)_{0.002}$-composites at 300°C in vacuum before cycling (a), after 500 cycles (b), and after 1000 cycles (c).

fastest desorption kinetics followed by VN and VC. Ultrapure metallic V shows no improvement over pure Mg with respect to reaction kinetics. However, kinetics can be successively improved towards Mg + VN/V_2O_5/VC by stepwise exposure to small amounts of air (Fig. 14).[29)] Additionally, some clues regarding the mechanism of catalysis can be drawn from the different catalytic activities of the investigated oxides. The metal oxides of this study can be devided into two groups: the first group consists of the oxides of the transition metals Ti, V, Cr, Mn, Fe, and Cu, in which the metal can have different valences. The second group are of the oxides Al_2O_3, SiO_2, and Sc_2O_3, in which the metal atom appears with only a single valence state. Because only the oxides of the first group have a catalytic effect, the ability of the metal atom to take different electronic states could play an important role with respect to the kinetics of the solid-gas-reaction.

An exception among the oxide catalysts is CuO. Though copper takes different valences in the respective oxides, it can be reduced easily by Mg due to its low stability of −156 kJ/g-atom-O and the negative heat of mixing between Mg and Cu.

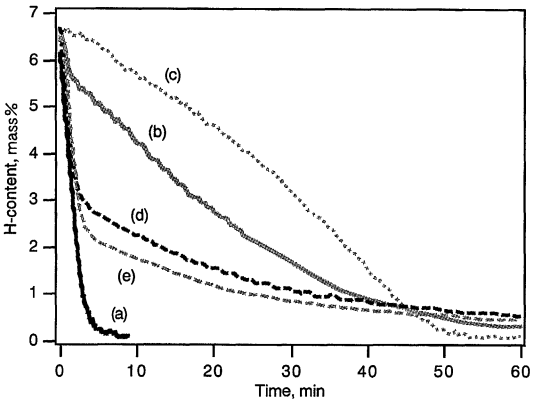

Fig. 14 Hydrogen desorption curves of as synthesized (a) $MgH_2/(V_2O_5)_{0.01}$, (b) $MgH_2/V_{0.01}$, (c) pure MgH_2, (d) the same material $MgH_2/V_{0.01}$ as in (b), but stored under Ar for 11 month, and (e) the same material $MgH_2/V_{0.01}$ as in (d) subsequently exposed to air for 17 h; each at 300°C in vacuum.

Upon repeated hydrogen sorption the intermetallic compound Mg_2Cu is formed beside MgO.[30] It is well known that Mg_2Cu has a catalytic effect on the absorption of Mg. In addition, it can be hydrided itself. This also explains the 2-step absorption of the material $MgH_2/(CuO)_{0.05}$ (Fig. 1(a)). In case of the other transition metal oxides, the heat of mixing between Mg and the transition metal is positive. Thus, there is no contribution to the reduction reaction of the oxides by the formation of intermetallic compounds during milling. This indicates that the thermodynamic stability of the oxides is critical.

For catalysis, the local electronic structure of the catalysts is also of great importance: before the dissociation of hydrogen molecules can take place, hydrogen has to be adsorbed at the surface of the catalyst. Regarding the sorption of hydrogen at TiO_2-surfaces (and other oxides not mentioned in this work), investigations of Henrich *et al.* have shown that (almost) perfect TiO_2-single-crystal-surfaces are inert towards reactions with H_2. However, H_2 is absorbed by TiO_2-surfaces that contain a higher density of defects in the crystal structure and thus also in the electronic surface structure.[31,32] Accordingly, the fast sorption kinetics of nanocrystalline MgH_2/Me_xO_y-systems may originate also from a very high defect density, introduced at the surface of the metal oxide particles during high energy ball milling.

4. Conclusions

High energy ball-milled MgH_2/Me_xO_y-nanocomposites (Me_xO_y = Sc_2O_3, TiO_2, V_2O_5, Cr_2O_3, Mn_2O_3, Fe_3O_4, CuO, Al_2O_3, SiO_2) were investigated with respect to hydrogen sorption kinetics, even at different temperatures. The transition-metal oxides act as catalysts for the magnesium-hydrogen reaction. Cr_2O_3 yields the fastest hydrogen absorption, whereas V_2O_5 and Fe_3O_4 cause the most rapid desorption of hydrogen. It is shown that the catalyst content can be at least as low as 0.2 mol%, *i.e.* 0.3 vol% or 1 mass% in the case of Cr_2O_3. The best metal oxide catalysts allow a hydrogen absorption at room temperature (p = 0.84 MPa) and a desorption at 200°C ($p \approx$ 0 MPa). Under these conditions the material's desorption rates fulfill the technical requirements for automotive applications.

Acknowledgments

This work is part of a cooperation between Hydro-Québec, Montreal (Canada), GfE Metals and Materials mbH, Nürnberg (Germany), and GKSS, Geesthacht (Germany). Discussions with V. Güther, R. Schulz, J. Huot, S. Boily, G. Liang, A. van Neste, and Z. Dehouche are gratefully acknowledged. This project is supported by the Bavarian Government.

REFERENCES

1) L. Belkbir, E. Joly and N. Gérard: Int. J. Hydrogen Energ. **6** (1981) 285–294.
2) B. Vigeholm, J. Kjoller, B. Larsen and A. S. Pedersen: J. Less-Common Met. **89** (1983) 135–144.
3) B. Bogdanovic, T. H. Hartwig and B. Spliethoff: Int. J. Hydrogen Energ. **18** (1993) 575–589.
4) B. Bogdanovic, K. Bohmhammel, B. Christ, A. Reiser, K. Schlichte, R. Vehlen and U. Wolf: J. Alloys Compd. **282** (1999) 84–92.
5) L. Zaluski, A. Zaluska, P. Tessier, J. O. Ström-Olsen and R. Schulz: Mater. Sci. Forum **225** (1996) 853.
6) P. Tessier, L. Zaluski, Z.-H. Yan, M. L. Trudeau, R. Bormann, R. Schulz and J. O. Ström-Olsen: Mater. Res. Soc. Symp. Proc. **286** (1993) 209–214.
7) M. L. Trudeau, R. Schulz, L. Zaluski, S. Hosatte, D. H. Ryan, C. B. Doner, P. Tessier, J. O. Ström-Olsen and A. Van Neste: *Proc. Int. Sym. Mechanical Alloying* **88–90**, ed. by P. H. Shingus, (Trans Tech Publications, Kyoto, Japan, 1991) pp. 537–544.
8) L. Zaluski, S. Hosatte, P. Tessier, D. H. Ryan, J. O. Ström-Olsen, M. L. Trudeau and R. Schulz: Z. Physikalische Chemie **183** (1994) 45–49.
9) L. Zaluski, A. Zaluska, P. Tessier, J. O. Ström-Olsen and R. Schulz: J. Alloy Compd. **227** (1995) 53–57.
10) G. Liang, S. Boily, J. Huot, A. Van Neste and R. Schulz: J. Alloys Compd. **267** (1998) 302–306.
11) G. Liang, S. Boily, J. Huot, A. Van Neste and R. Schulz: J. Alloys Compd. **268** 1998) 302–307.
12) K. J. Gross, P. Spatz, A. Züttel and L. Schlapbach:. J. Alloys Compd. **240** (1996) 206–213.
13) W. Oelerich: PhD thesis, Technical University Hamburg-Harburg, (2000) in German.
14) A. L. Reimann: Philos. Mag. **16** (1933) 673–686.
15) E. Fromm and H. Uchida: J. Less-Common Met. **131** (1987) 1–12.
16) H. H. Uchida, H.-G. Wulz and E. Fromm: J. Less-Common Met. **172** (1991) 1076–1083.
17) L. Zaluski, A. Zaluska, P. Tessier, J. O. Ström-Olsen and R. Schulz: J. Alloys Compd. **217** (1995) 295–300.
18) L. Zaluski, A. Zaluska, P. Tessier, J. O. Ström-Olsen and R. Schulz: J. Mater. Sci. **31** (1996) 695–698.
19) B. Tanguy, J.-L. Soubeyroux, M. Pezat, J. Portier and P. Hagenmüller: Mater. Res. Bull. **11** (1976) 1441–1448.
20) G. Liang, J. Huot, S. Boily, A. Van Neste and R. Schulz: J. Alloys Compd. **291** (1999) 295–299.
21) G. Liang, J. Huot, S. Boily, A. Van Neste and R. Schulz: J. Alloys Compd. **292** (1999) 247–252.
22) R. Schulz, S. Boily and J. Huot: Canadian patent, Ser.-Nr.: 2207149, (1999).
23) C. Liu, Y. Y.Fan, M. Liu, H. T. Cong, H. M. Cheng and M. S. Dresselhaus: Science **286** (1999) 1127–1129.
24) W. Oelerich, T. Klassen and R. Bormann: J. Alloys Compd. **315** (2001) 237–242.
25) K. Zeng, T. Klassen, W. Oelerich and R. Bormann: Int. J. Hydrogen Energ. **24** (1999) 989–1004.
26) G. Liang, J. Huot, S. Boily, A. Van Neste and R. Schulz: J. Alloys Compd. **297** (2000) 261–265.
27) W. Oelerich, Z. Dehouche, T. Klassen, R. Bormann and R. Schulz: unpublished.
28) Daimler Chrysler: private communication.
29) W. Oelerich, T. Klassen and R. Bormann: J. Alloys Compd. **322** (2001) L5–L9.
30) J. J. Reilly and R. H. Wiswall: Inorg. Chem. **6** (1967) 2220–2223.
31) V. Henrich: Prog. Surf. Sci. **9** (1979) 143.
32) V. Henrich: Rep. Prog. Phys. **48** (1985) 1481.
33) M. Y. Song: Int. J. Hydrogen Energ. **20** (1995) 221–227.